Available online at www.sciencedirect.com
SCIENCE DIRECT®
Chemical Physics Letters 411 (2005) 350–356
CHEMICAL PHYSICS LETTERS
www.elsevier.com/locate/cplett

Ionization and dissociation of simple molecular ions in intense infrared laser fields: Quantum dynamical simulations for three-dimensional models of HD^+ and H_2^+

G.K. Paramonov [a,b,*]

[a] Institut für Chemie – Physikalische und Theoretische Chemie, Freie Universität Berlin, Takustrasse 3, 14195 Berlin, Germany
[b] National Academy of Sciences of Belarus, Institute of Physics, Skaryna Avenue 70, 220602 Minsk, Republic of Belarus

Received 29 March 2005; in final form 13 June 2005
Available online 5 July 2005

Abstract

The dynamics of multiphoton excitation of HD^+ and H_2^+ in quasi-resonant infrared intense laser fields ($I_0 = 1.18 \times 10^{14}$ W/cm^2) is studied by the numerical solution of the time-dependent Schrödinger equations for the systems with explicit treatment of the nuclear vibrations and the electron motion beyond the Born–Oppenheimer approximation. It has been found, in particular, that on the time scale of 400 fs the overall ionization yield is about 40% for HD^+, but only about 0.45% for H_2^+ while in accordance with the tunnel (or field) ionization mechanism at least comparable ionization yields could be expected for HD^+ and H_2^+. The physical reason for this remarkable difference is that the nuclear motion is excited directly by the strong infrared laser field in HD^+, but not in H_2^+.

1. Introduction

Systematic investigations of molecules in intense ($I_0 > 10^{13}$ W/cm^2) laser fields carried out in the last decade already led to the discovery of such new phenomena as above threshold ionization and dissociation [1,2], bond softening [3,4] and bond hardening [5,6], and ionization using near-infrared laser pulses [7,8]. The problem continues to attract ever-increasing attention now due to the development of laser systems generating highly intense ($I_0 > 10^{16}$ W/cm^2) ultrashort pulses [9,10], which provide new tools for manipulating the molecular dynamics on the femtosecond (fs) time scale [11], such as controlling the branching ratios of different dissociation channels [12,13] and selective bond dissociation and rearrangement of polyatomic molecules [14].

Of special theoretical interest are molecular ions H_2^+ and HD^+, the basic systems representing homonuclear and heteronuclear diatomic molecules. Their relative simplicity allows to treat both nuclear and electronic motion explicitly, beyond the Born–Oppenheimer approximation [15–18]. In particular, a three-dimensional (3-D) quantum dynamics of H_2^+ in strong laser fields ($I_0 > 10^{13}$ W/cm^2) in the ultraviolet and near-infrared domains has been studied by Bandrauk, Fujimura, Kono and their coworkers [15–18].

Excitation of H_2^+ and HD^+ by the quasi-resonant infrared (IR) laser fields is especially interesting for the following reasons. Firstly, if the Born–Oppenheimer approximation be employed, H_2^+ could not be excited at all. On the other hand, H_2^+ and HD^+ differ only by the mass of one nucleus, therefore the electron response to the IR field should be similar in both systems. Thirdly, the IR laser field can excite the nuclear vibrations in HD^+ directly, therefore a comparative study of H_2^+ and HD^+ makes it possible to reveal the role of the nuclear motion in the ionization process.

* Fax: +49 30 838 54792.
E-mail address: paramon@chemie.fu-berlin.de.

0009-2614/$ - see front matter © 2005 Elsevier B.V. All rights reserved.
doi:10.1016/j.cplett.2005.06.047

2. Model

The systems under study are represented usually in terms of a 3-D model shown in Fig. 1 for HD^+. Here, the applied laser field is assumed to be linearly polarized along the z-axis; the nuclear motion is restricted to the polarization direction of the laser electric field, whereas the electron moves in three dimensions with conservation of cylindrical symmetry. Accordingly, only two electron coordinates, z and ρ, measured with respect to the center of mass of the two nuclei, should be treated explicitly together with the internuclear distance R. Note, that in several cases, simpler models with a reduced dimensionality, e.g., fixed internuclear distance, electronic motion only along the z-axis, can be employed as well [19–22].

The present work is addressed to the 3-D quantum dynamics of H_2^+ and HD^+ in strong ($I_0 = 1.18 \times 10^{14}$ W/cm^2) quasi-resonant IR laser fields which can efficiently excite not only electronic motion in both systems, but also nuclear vibrations in HD^+. The component of the dipole moment of HD^+ along the z-axis reads [23]

$$d_z(R,z) = -e[R(m_D - m_H)/M + z(1 + m_e/\mathscr{M})], \quad (1)$$

where e is the electron charge, $M = m_D + m_H$, $\mathscr{M} = M + m_e$, and m_D, m_H and m_e are the nuclear and the electron masses, respectively. Due to the dipole moment, vibrational motion in HD^+ can be excited directly by the IR laser field, and also indirectly due to the electron motion. The H_2^+ ion does not have a permanent dipole moment,

$$d_z(z) = -ez(1 + m_e/\mathscr{M}), \quad (2)$$

and its vibrational motion can be excited only indirectly, i.e., due to the electron motion. Moreover, vibrational motion in HD^+ can result in substantial delocalization of the electron wave packet, and this should change the electronic response to the field, e.g., the ionization probability, as compared to H_2^+.

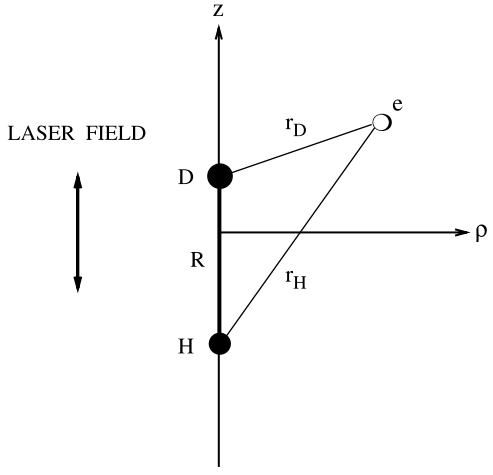

Fig. 1. The 3-D model of HD^+ excited by a laser field linearly polarized along the z-axis. The internuclear distance is R, the distances between the electron and each of the two nuclei are r_H and r_D, see Eqs. (6) and (7).

In the present model simulations, a continuous-wave (CW) laser field

$$\mathscr{E}(t) = \mathscr{E}_0 \sin(\omega t) \quad (3)$$

is used, which is switched on at $t = 0$, and is assumed to be linearly polarized along the z-axis (see Fig. 1). The laser field amplitude is $\mathscr{E}_0 = 2.98 \times 10^2$ MV/cm, the laser frequencies are chosen close (but not equal) to the corresponding frequencies of the $|v = 0\rangle \rightarrow |v = 1\rangle$ transitions: $\omega = 1909$ cm^{-1} for HD^+ and $\omega = 2322$ cm^{-1} for H_2^+. The adiabaticity parameter γ calculated with the original Keldysh's theory [24] is $\gamma = 0.22$ for HD^+ and $\gamma = 0.26$ for H_2^+, therefore at least comparable ionization yields for HD^+ and H_2^+ can be expected in accordance with the tunnel (or field) ionization mechanism. Note, that the adiabaticity parameters are given here as a reference only; generalization of Keldysh's theory for atoms and molecules is discussed in [25–27].

3. Equations of motion and technique

The time-dependent Schrödinger equation (TDSE) for the three-body 3-D model of HD^+ in the classical laser field (see Fig. 1) can be written in the following form:

$$i\hbar\frac{\partial}{\partial t}\Psi = -\frac{\hbar^2}{2\mu_n}\frac{\partial^2\Psi}{\partial R^2} - \frac{\hbar^2}{2\mu_e}\left(\frac{\partial^2\Psi}{\partial\rho^2} + \frac{1}{\rho}\frac{\partial\Psi}{\partial\rho}\right) - \frac{\hbar^2}{2\mu_e}\frac{\partial^2\Psi}{\partial z^2} + V_C(R,\rho,z)\Psi - d_z(R,z)\mathscr{E}(t)\Psi, \quad (4)$$

where $\mu_n = m_H m_D/M$ is the nuclear reduced mass, $\mu_e = m_e M/\mathscr{M}$, is the electron reduced mass; the Coulomb potential reads

$$V_C(R,\rho,z) = e^2(1/R - 1/r_H - 1/r_D), \quad (5)$$

where the electron–proton distance is

$$r_H(R,\rho,z) = [\rho^2 + (z + m_D R/M)^2]^{1/2} \quad (6)$$

and the electron–deuteron distance is

$$r_D(R,\rho,z) = [\rho^2 + (z - m_H R/M)^2]^{1/2}. \quad (7)$$

The dipole moment $d_z(R,z)$ and the CW laser field $\mathscr{E}(t)$ in Eq. (4) are defined by Eqs. (1) and (3). The wave function $\Psi(R,\rho,z,t)$ in Eq. (4) is normalized with the elementary volume $\rho\,dR\,d\rho\,dz$.

In the case of H_2^+, the nuclear mass m_D is replaced by m_H, and the straightforward modifications of Eqs. (4)–(7) result in the equation of motion solved numerically in [15–17]. Bandrauk and his coworkers [15] employed the Bessel–Fourier expansion [19] in the ρ variable and solved the resulting system of differential equations with the split operator technique together with fast Fourier

transform (FFT) in the z and R variables. Fujimura, Kono and Kawata [16,17] made use of the variable transformations in the ρ and z coordinates (spatial derivatives were evaluated by the finite difference method) and employed the alternating-direction implicit (ADI) method for the time-propagation.

In the present work, the IR-laser excitation of HD^+ and H_2^+ is studied. Therefore it is desirable to employ the propagation technique which is fast enough to cover many cycles of the field and accurate enough to calculate the dissociation and ionization yields even if they are small (as for H_2^+). Basically, the variable transformation $y = f(\rho)$ is used in the ρ coordinate, afterwards the Laguerre expansion in the y coordinate and the Hermite expansion in the z coordinate are employed, as described below, in order to account for all terms containing spatial derivatives related to the electronic motion. Finally, the split operator propagation method is used together with FFT for the nuclear R coordinate.

First, the wave function $\Psi(R,\rho,z,t)$ of Eq. (4) is represented as

$$\Psi(R,\rho,z,t) = \sqrt{\rho}\Upsilon(R,\rho,z,t). \tag{8}$$

Substitution of Eq. (8) into Eq. (4) gives the equation of motion for $\Upsilon(R,\rho,z,t)$, where the variable transformation $\rho = 2y^{1/2}$ is made, yielding $\Upsilon(R,\rho,z,t) \Rightarrow \Omega(R,y,z,t)$ and the corresponding equation for $\Omega(R,y,z,t)$. Therein, the wave function $\Omega(R,y,z,t)$ is represented as

$$\Omega(R,y,z,t) = y^{\frac{1}{4}} e^{-(y+z^2)/2}\Phi(R,y,z,t), \tag{9}$$

which gives finally the following equation of motion for $\Phi(R,y,z,t)$:

$$\begin{aligned} i\hbar\frac{\partial}{\partial t}\Phi = &-\frac{\hbar^2}{2\mu_n}\frac{\partial^2\Phi}{\partial R^2} - \frac{\hbar^2}{2\mu_e}\left[y\frac{\partial^2\Phi}{\partial y^2} + (1-y)\frac{\partial\Phi}{\partial y}\right] \\ &+ \frac{\hbar^2}{2\mu_e}\left(\frac{1}{2} - \frac{y}{4}\right)\Phi - \frac{\hbar^2}{2\mu_e}\left(\frac{\partial^2\Phi}{\partial z^2} - 2z\frac{\partial\Phi}{\partial z}\right) \\ &+ \frac{\hbar^2}{2\mu_e}(1-z^2)\Phi + V_C(R,y,z)\Phi \\ &- d_z(R,z)\mathscr{E}(t)\Phi. \end{aligned} \tag{10}$$

The wave function $\Phi(R,y,z,t)$ in Eq. (10) is normalized with the elementary volume $e^{-y-z^2}\,dR\,dy\,dz$.

It is easy to recognise in the right-hand side of Eq. (10) parts of the differential equations for the Laguerre polynomials $L_m(y)$ and the Hermite polynomials $H_n(z)$, respectively [28]:

$$y\frac{\partial^2 L_m(y)}{\partial y^2} + (1-y)\frac{\partial L_m(y)}{\partial y} = -mL_m(y), \tag{11}$$

$$\frac{\partial^2 H_n(z)}{\partial z^2} - 2z\frac{\partial H_n(z)}{\partial z} = -2nH_n(z). \tag{12}$$

Therefore, the polynomial expansion can be efficiently used here, thus accounting for all terms containing spatial derivatives with respect to both $y = f(\rho)$ and z coordinates related to the electronic motion. The respective part of the propagation can be accomplished as follows. Expanding the wave function $\Phi(R,y,z,t)$ in the polynomial series

$$\Phi(R,y,z,t) = \sum_{k,l} A_{k,l}(R,t)L_k(y)H_l(z), \tag{13}$$

inserting Eq. (13) into Eq. (10), making use of Eqs. (11) and (12) and operating, as usual, with $L_m(y)H_n(z)$ and their weights, one gets the following equation for the amplitudes $A_{m,n}(R,t)$:

$$i\frac{d}{dt}A_{m,n}(R,t) = \frac{\hbar(m+2n)}{2\mu_e}A_{m,n}(R,t), \tag{14}$$

wherein the nuclear variable R is treated as a parameter, with the obvious solution

$$A_{m,n}(R,t+\Delta t) = A_{m,n}(R,t)\exp\left[-i\frac{\hbar(m+2n)\Delta t}{2\mu_e}\right]. \tag{15}$$

Note, that propagator (15) depends only linearly on both numbers of the grid-points for the electronic motion (not quadratically as in the case of FFT, for example). Therefore, a high accuracy can be achieved even at rather large values of the time step of the propagation Δt. The time step, $\Delta t = 0.04$ a.u., is used throughout this paper due to a relatively small dissociation and ionization probabilities of H_2^+ (see the next Section).

The calculations for the electronic motion have been performed by making use of IMSL routines which provide non-equidistant grids for polynomials $L_m(y)$ and $H_n(z)$, together with corresponding weights for the numerical integration on the interval $(0,\infty)$ for the $y = f(\rho)$ coordinate and on the interval $(-\infty,\infty)$ for the z coordinate (details will be reported elsewhere). For the nuclear coordinate R, the 256-point equidistant grid has been used on the interval from $R_{min} = 0.12a_0$ to $R_{max} = 16.7a_0$ (a_0 stands for the Bohr radius). In order to damp the 3-D wave packet at the outer ends of the spatial grids, the absorbing boundary conditions have been provided by the imaginary smooth optical potentials [29,30]. The dissociation probability P_D has been calculated with the time- and space-integrated outgoing flux for the nuclear coordinate R, while the ionization probabilities have been calculated with the respective fluxes separately for the positive and the negative direction of the z-axis (denoted as $P_I(+)$ and $P_I(-)$, respectively) as well as for the outer end of the ρ-axis, denoted as $P_I(\rho)$.

The parameters of the imaginary optical potentials (the widths and the depths) have been chosen such that the results were not sensitive to their variations. Specifically, the depth of the imaginary potential was 0.15 a.u. for the nuclear coordinate R, and 3.3 a.u. for the electron coordinates z and ρ. The widths of the optical potentials along the R, z and ρ coordinates were chosen such that the 3-D wave packet was damped at

$R > 13.9a_0$, at $z < -14.2a_0$ and $z > 14.2a_0$, and at $\rho > 14.4a_0$.

4. Excitation, dissociation and ionization of HD^+ and H_2^+ in the IR laser fields

Initially, at $t = 0$, both HD^+ and H_2^+ are assumed to be in their ground vibrational and ground electronic states. The wave functions of the initial states have been obtained by the numerical propagation of TDSE (10) for HD^+ and the respective equation of motion for H_2^+ in imaginary time.

The 3-D quantum dynamics of HD^+ is illustrated in the upper panel of Fig. 2 with the time-dependent population of the initial ground state, $P_{v=0}(t)$, the expectation value of the z component of the dipole moment, $\langle d_z(t)\rangle$ (in atomic units, a.u.), and the expectation value of the overall energy of the system, $\langle E(t)\rangle$ (in a.u.). With the applied IR laser field being linearly polarized along the z-axis (see Fig. 1), the expectation value $\langle d_z(t)\rangle$ represents effects of both the nuclear motion along R and the electron motion along the z-axis, see Eq. (1). The population of the vibrational ground state accounts for the vibrational excitation, implying also variation of the bond length: for example, the local minima of curve '$P_{v=0}$' imply that HD^+ is vibrationally excited and the HD bond is stretched and vice versa. In the lower panel of Fig. 2, the applied IR laser field is shown, comprising eight optical cycles on the time scale of 140 fs.

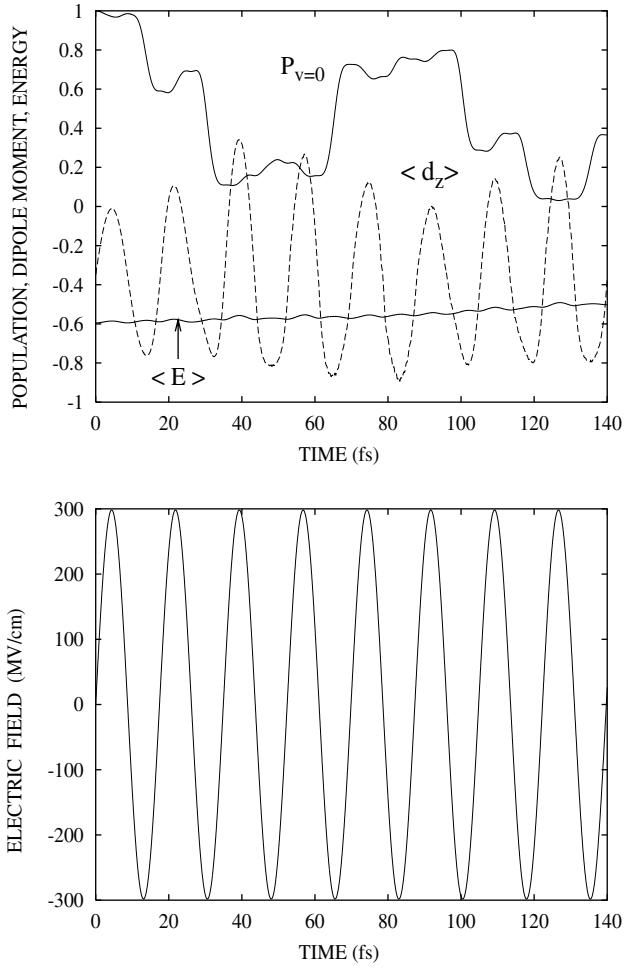

Fig. 2. HD^+ in the IR laser field. Upper panel: the population of the ground state (curve '$P_{v=0}$'), the z component of the dipole moment (curve '$\langle d_z\rangle$', a.u.), and the mean energy (curve '$\langle E\rangle$', a.u.). Lower panel: the IR laser field with $\mathscr{E}_0 = 2.98 \times 10^2$ MV/cm and $\omega = 1909\ \mathrm{cm}^{-1}$.

Analysis of Fig. 2 shows that the electron motion along the z coordinate is correlated with both the applied IR laser field and the nuclear motion. First, the electron wave packet follows the laser field: the maxima and the minima of $\langle d_z(t)\rangle$ coincide with those of the field. At the same time, the field-following fast electronic oscillations are modulated by a relatively slow nuclear motion: the amplitude of the electronic fast oscillations increases periodically with the vibrational excitation of HD^+ and its bond length, corresponding to the local minima of the population of the vibrational ground state (curve '$P_{v=0}$'). In contrast, when the vibrational energy is relatively small and the HD bond is contracted (the local maxima of curve '$P_{v=0}$'), the amplitude of the field-following fast electronic oscillations is relatively small, too.

Basically, the electron demonstrates a dual motion. Being coupled to the nuclei by the Coulombic attraction, it follows the nuclear motion, which in the case of HD^+ is excited directly by the IR laser field: the electron wave packet is delocalized along the z-axis when the HD bond is stretched and localized in a narrower domain when the bond is contracted. At the same time, being coupled to the IR field, the electron follows the relatively fast oscillations of the field: the electron wave packet is transferred from one nucleus to the other four times at the turning points of the nuclear vibrations, when the HD bond is either stretched or contracted (each transfer being accomplished within a half optical cycle). The expectation value of the overall energy of HD^+ (see curve '$\langle E\rangle$') increases from the initial value of -0.5951 a.u. to -0.5021 a.u. at $t = 140$ fs. As it could be expected, the energy $\langle E(t)\rangle$ has local maxima corresponding to each maximum delocalization of the electronic wave packet (in either positive or negative direction of the z-axis).

The 3-D quantum dynamics of H_2^+ in the IR laser field is presented in Fig. 3. In contrast with HD^+, the dipole moment of H_2^+ does not depend on the internuclear distance R at all, see Eqs. (1) and (2). The nuclear motion of H_2^+ is, therefore, activated only by the fast field-following oscillations of the electron. Periodic shifts of the electron density to one of the two nuclei disturb the equilibrium configuration of the entire system and result in the Coulombic repulsion of the other nucleus. In a half optical cycle the situation changes to

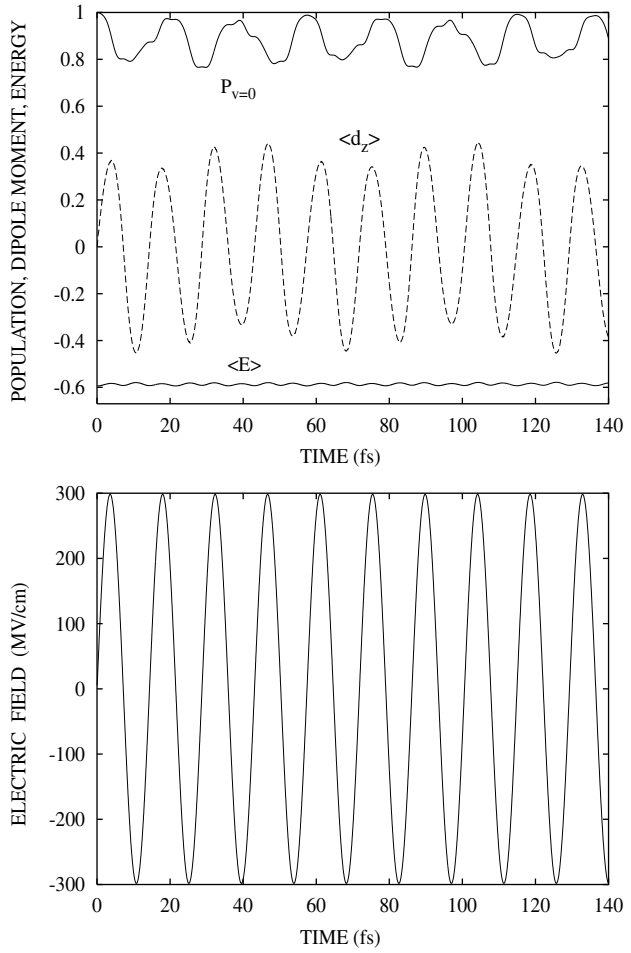

Fig. 3. H_2^+ in the IR laser field. Upper panel: the population of the ground state (curve '$P_{v=0}$'), the z component of the dipole moment (curve '$\langle d_z\rangle$', a.u.), and the mean energy (curve '$\langle E\rangle$', a.u.). Lower panel: the IR laser field with $\mathscr{E}_0 = 2.98 \times 10^2$ MV/cm and $\omega = 2322\ \mathrm{cm}^{-1}$.

the opposite, etc. A similar process also takes place in HD^+, but the direct excitation of the nuclear motion by the IR laser field dominates. It is seen from Fig. 3, that the population of the vibrational ground state of H_2^+ changes periodically by about 20%, implying the respective change of the vibrational energy, which can be estimated as quite a considerable variation, taking into account that within the Born–Oppenheimer approximation H_2^+ cannot be vibrationally excited at all. Being activated by the electronic motion, nuclear vibrations of H_2^+ influence the electronic motion as well, and the fast field-following oscillations are modulated by a relatively slow nuclear motion, though not as strongly as in HD^+. The expectation value of the overall energy of H_2^+ (see curve '$\langle E\rangle$' in Fig. 3) increases from the initial value of -0.5942 a.u. to -0.5806 a.u. at $t = 140$ fs and has local maxima corresponding to every maximum delocalization of the electronic wave packet along the z-axis (in either its positive or negative direction).

The relatively slow oscillations of the dipole moment $\langle d_z(t)\rangle$, which are seen in Figs. 2 and 3, can be explained as follows. On the contrary to the electron, the relatively heavy nuclei do not follow the oscillations of the laser field. In H_2^+, for example, the period of the nuclear vibrations τ_{nu} is approximately 19 fs (see curve '$P_{v=0}$' in Fig. 3) implying the nuclear frequency $\omega_{\mathrm{nu}} \approx 1751\ \mathrm{cm}^{-1}$, while the applied laser frequency is $\omega = 2322\ \mathrm{cm}^{-1}$ (the period is $\tau = 14.33$ fs). Being coupled to both the applied laser field and the nuclear motion, the electron demonstrates the superposition of the two oscillations with the frequencies ω and ω_{nu}, respectively, which can always be represented as the oscillation with the laser frequency ω modulated with the difference frequency $\Delta\omega_{\mathrm{nu}} = \omega - \omega_{\mathrm{nu}}$. A simple model example reads

$$\sin(\omega t) + \alpha_{\mathrm{nu}} \sin(\omega_{\mathrm{nu}} t) = [1 + \alpha_{\mathrm{nu}} \cos(\Delta\omega_{\mathrm{nu}} t)] \sin(\omega t) - \alpha_{\mathrm{nu}} \sin(\Delta\omega_{\mathrm{nu}} t) \cos(\omega t), \quad (16)$$

where $\alpha_{\mathrm{nu}} < 1$ due to a small amplitude of the nuclear vibrations as compared to the amplitude of the field-following electronic oscillations. In H_2^+, for example, the period corresponding to the difference frequency $\Delta\omega_{\mathrm{nu}}$ is approximately 58 fs. This value is in a good agreement with the period of the slow oscillation of the dipole moment of H_2^+ (see curve '$\langle d_z\rangle$' in Fig. 3). A similar process takes place in HD^+ as well.

It is also seen from Figs. 2 and 3, that sharp changes of the vibrational energy of H_2^+ and HD^+ are often accomplished within a half optical cycle of the IR laser field. Therefore, specially designed half-cycle pulses can be efficiently used to control, for example, the state-selective population transfer in H_2^+ and HD^+ as well as dissociation. This approach will be addressed to in a separate work.

The fast field-following oscillation of the electron density result in a stepwise manner of the ionization from both positive and negative direction of the z-axis. The time-dependent ionization and dissociation probabilities of HD^+ and H_2^+ are shown in Figs. 4 and 5, correspondingly, on the time scale of 400 fs. When the electron density is transferred, for example, to the positive end of the z-axis, ionization takes place there and the respective ionization probability $P_{\mathrm{I}}(+)$ increases stepwisely, while at the negative end of the z-axis the respective ionization probability $P_{\mathrm{I}}(-)$ remains constant due to a very small electron density there. In a half optical cycle the electron density is transferred to the negative end of the z-axis, and the situation changes to the opposite: ionization probability $P_{\mathrm{I}}(-)$ increases stepwisely, while at the positive end of the z-axis $P_{\mathrm{I}}(+)$ remains constant, etc. Thus, during each optical cycle of the field, two steps of the ionization occur from alternate ends of the z-axis. Close analysis of Fig. 4 shows that the ionization from the outer end of the ρ-axis, $P_{\mathrm{I}}(\rho)$, also proceeds in a stepwise manner, but here, every step corresponds to every half cycle of the field, i.e., to every turning point of the electron motion along the z-axis.

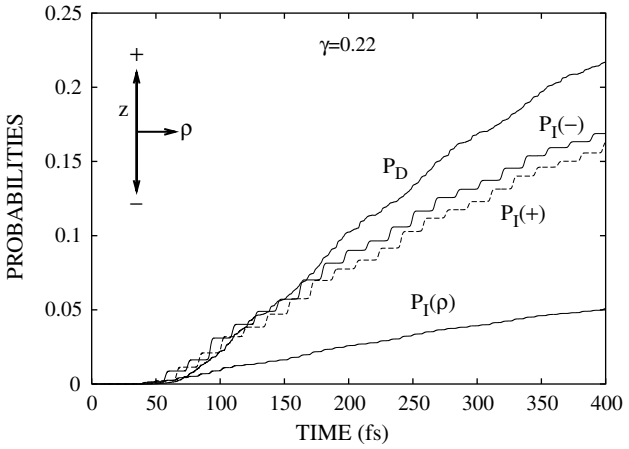

Fig. 4. Time-dependent dissociation and ionization probabilities of HD^+ excited by the IR-laser field linearly polarized along the z-axis: P_D is the dissociation probability, $P_I(+)$ (the dashed line) is the ionization probability from the positive direction of the z-axis, $P_I(-)$ is the ionization probability from the negative direction of the z-axis, $P_I(\rho)$ is the ionization probability from the positive direction of the ρ-axis (see the insert in the upper-left corner herein and also Fig. 1). The Keldysh parameter is $\gamma = 0.22$.

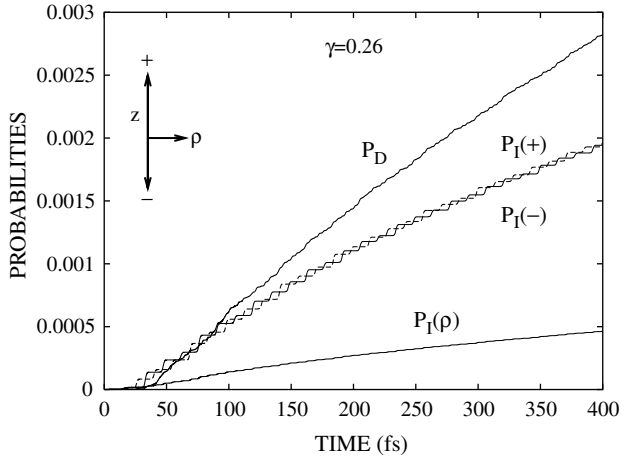

Fig. 5. Time-dependent dissociation and ionization probabilities of H_2^+ excited by the IR-laser field linearly polarized along the z-axis (the labelling is as in Fig. 4). The Keldysh parameter is $\gamma = 0.26$.

Note also, that for both HD^+ and H_2^+, the ionization probability from the outer end of the ρ-axis at $t = 400$ fs is approximately three times smaller that those from the outer ends of the z-axis (it is not negligibly small). Thus, even though the applied IR laser field is polarized along the z-axis, the electronic density is substantially delocalized in the perpendicular direction as well.

Comparison of Figs. 4 and 5 shows that although both ionization and dissociation probabilities of HD^+ are almost two orders of magnitude larger than those of H_2^+, the dynamics of these processes are similar for both systems, and the interrelation of the ionization and dissociation can be described as follows. Due to the very small electron mass, the electron density follows the oscillations of the applied field, evolving much faster than the nuclear one, and therefore the ionization starts prior to the dissociation in both HD^+ and H_2^+. Each step of the ionization decreases slightly the negative charge between the two nuclei which thus become slightly more repulsive. This results in the vibrational excitation of the molecule during each half optical cycle and eventually in the dissociation facilitated by the ionization. It is seen from Figs. 4 and 5 (curves 'P_D') that the dissociation also occurs in a stepwise manner, and every step of it corresponds to every half cycle of the field. The vibrational excitation, in turn, facilitates the ionization, because the elongation of the internuclear distance R increases the delocalization of the electron density along the z axis (see Fig. 1). Thus, the vibrational excitation and the ionization facilitate each other. For this reason, both ionization and dissociation probabilities of HD^+, where the nuclear motion is excited by the IR laser field directly, are much higher than those of H_2^+.

The important role played by the nuclear motion in the process of molecular ionization is also seen from the comparison of the ionization yields of HD^+ and H_2^+ from the positive and the negative directions of the z-axis, represented in Figs. 4 and 5 by curves '$P_I(-)$' and '$P_I(+)$', respectively. In HD^+, due to the small mass of the proton as compared to the deuteron, the proton displacement in the negative direction of the z axis is larger than the deuteron displacement in the positive direction of the z-axis (see Fig. 1). Being coupled to the nuclei by the Coulombic attraction and thus following the nuclear motion, the electron density in HD^+ is delocalized accordingly: more to the negative and less to the positive direction of the z-axis. Therefore, as it is seen from curves '$P_I(-)$' and '$P_I(+)$' in Fig. 4, the ionization yield in the negative direction of the z-axis is higher than that in the positive direction. In contrast, H_2^+ has two nuclei with the same masses, so that the ionization probabilities $P_I(-)$ and $P_I(+)$ are very close to each other, see Fig. 5.

5. Conclusion

A comparative investigation of the 3-D quantum dynamics of HD^+ and H_2^+ excited by quasi-resonant IR laser fields performed in this work demonstrates the important role played by the vibrational excitation of the molecule in its ionization and reveals the interrelation of the electronic motion (eventually resulting in ionization) and the vibrational excitation (eventually resulting in dissociation) which facilitate each other. Being coupled to the IR laser field, the electron demonstrates fast field-following oscillations and simultaneously follows the nuclear motion due to the Coulombic attraction. Periodic displacement of the

electron density during the field-following oscillations decreases the negative charge between the two nuclei whenever the electron is at its turning points, causing periodic repulsion of the nuclei. This results in the vibrational excitation of the system together with the corresponding elongation of its bond. The elongation of the internuclear distance, in turn, increases the delocalization of the electron density during the field-following oscillations and thus increases the ionization probability, which in turn, increases the vibrational excitation and the dissociation probability. Since the strong quasi-resonant IR laser field can excite the nuclear motion of HD^+ also directly (in contrast with H_2^+), both dissociation and ionization probabilities of HD^+ are almost two orders of magnitude larger than those of H_2^+.

A strong increase of the ionization rates of H_2^+, which was assumed to be vibrationally excited initially to $v = 3$ and $v = 6$ of the ground electronic state, and subjected to the UV laser fields with $\lambda = 228$ nm and $\lambda = 212$ nm, was evaluated numerically in [19,15]. The enhanced ionization was explained therein by the fact that the upper repulsive state σ_u (where the probability for the electron to stay between the nuclei becomes small compared to that in the ground electronic state) can be reached with one-photon resonance transitions from the vibrationally excited states of H_2^+ and only with two-photon transition from its ground vibrational state.

The excitation with the IR laser field studied in the present work does not provide such a high vibrational excitation of H_2^+ as $v = 3$ and $v = 6$, and the upper state σ_u is not involved at all. The high ionization probability of HD^+ is not related to any specific vibrational state (which just cannot be prepared selectively with the CW laser field used here) and explained by the interrelation of the nuclear motion and the electronic motion, as described at the beginning of this Section.

Acknowledgements

This work was supported by the Alexander von Humboldt-Stiftung through the Humboldt Research Award, which is gratefully acknowledged. I would also like to thank Prof. K.-L. Kompa (MPI Garching) and Prof. J. Manz (FU Berlin) for very stimulating discussions. The computer simulations of molecular dynamics were performed on a HP J6700 workstation and on HP rx2600 servers at the Freie Universität Berlin.

References

[1] A. Guisti-Suzor, X. He, O. Atabek, Phys. Rev. Lett. 64 (1990) 515.
[2] A. Bandrauk, J. Gauthier, J. Opt. Soc. Am. B 7 (1990) 1422.
[3] A. Bandrauk (Ed.), Molecules in Laser Fields, Marcel Dekker, New York, 1994.
[4] P. Bucksbaum, A. Zavrijev, H. Muller, D. Schumacher, Phys. Rev. Lett. 64 (1990) 1883.
[5] G. Yao, S.-I. Chu, Phys. Rev. A 48 (1993) 485.
[6] L. Frasinski, J. Posthumus, J. Plumridge, E. Charron, B. Yang, Phys. Rev. Lett. 83 (1999) 3625.
[7] M.J. DeWitt, R.J. Levis, J. Chem. Phys. 102 (1995) 8670.
[8] M.J. DeWitt, D.W. Peters, R.J. Levis, Chem. Phys. 218 (1997) 211.
[9] T. Brabec, F. Krausz, Rev. Mod. Phys. 72 (2000) 545.
[10] M. Hentschel, R. Kienberger, C. Spielmann, G.A. Reider, N. Milosevic, T. Brabec, P. Corkum, U. Heinzmann, M. Drescher, F. Krausz, Nature 414 (2001) 509.
[11] A. Bandrauk, Y. Fujimura, R. Gordon (Eds.), Laser Control and Manipulation of Molecules, ACS Symposium Series 821, American Chemical Society, Washington, DC, 2002.
[12] A. Assion, T. Baumert, M. Bergt, T. Brixner, B. Kiefer, V. Seyfried, M. Strehle, G. Gerber, Science 282 (1998) 919.
[13] T. Brixner, G. Gerber, Chem. Phys. Phys. Chem. 48 (2003) 418.
[14] R.J. Levis, G.M. Menkir, H. Rabitz, Science 292 (2001) 709.
[15] S. Chelkowski, T. Zuo, O. Atabek, A.D. Bandrauk, Phys. Rev. A 52 (1995) 2977.
[16] I. Kawata, H. Kono, Y. Fujimura, J. Chem. Phys. 110 (1999) 11152.
[17] I. Kawata, H. Kono, J. Chem. Phys. 111 (1999) 9498.
[18] H. Kono, Y. Sato, N. Tanaka, T. Kato, K. Nakai, S. Koseki, Y. Fujimura, Chem. Phys. 304 (2004) 203.
[19] S. Chelkowski, T. Zuo, A.D. Bandrauk, Phys. Rev. A 46 (1992) R5342.
[20] A.D. Bandrauk, S. Chelkowski, Phys. Rev. Lett. 84 (2000) 3562.
[21] A.D. Bandrauk, S. Chelkowski, Phys. Rev. Lett. 87 (2001) 2730.
[22] T. Kreibich, R. van Leeuwen, E.K.U. Gross, Chem. Phys. 304 (2004) 183.
[23] A. Carrington, I.R. McNab, C.A. Montgomerie, J. Phys. B: At. Mol. Opt. Phys. 22 (1989) 3551.
[24] L.V. Keldysh, Sov. Phys. JETP 20 (1965) 1307.
[25] K. Mishima, M. Hayashi, J. Yi, H. Lin, H.L. Selzle, E.W. Schlag, Phys. Rev. A 66 (2002) 033401, 053408.
[26] M.J. DeWitt, R.J. Levis, Phys. Rev. Lett. 81 (1998) 5101.
[27] M.J. DeWitt, R.J. Levis, J. Chem. Phys. 108 (1998) 7739.
[28] I.S. Gradshtein, I.M. Ryzhik, Table of Integrals, Series, and Products, Academic Press, New York, 1980.
[29] Á. Vibók, G.G. Balint-Kurti, J. Chem. Phys. 96 (1992) 7615.
[30] Á. Vibók, G.G. Balint-Kurti, J. Phys. Chem. 96 (1992) 8712.